Alexandria Engineering Journal (2020) 59, 4969–4983

HOSTED BY ELSEVIER

Alexandria University

Alexandria Engineering Journal

www.elsevier.com/locate/aej
www.sciencedirect.com

Multi-objective optimal design of hybrid composite laminates under eccentric loading

Bertan Beylergil

Mechanical Engineering Department, Alanya Alaaddin Keykubat University, Alanya, Antalya 07450, Turkey

Received 14 March 2019; revised 9 September 2020; accepted 12 September 2020
Available online 25 September 2020

KEYWORDS

Genetic algorithms;
Hybrid composites;
Optimization;
Eccentric loading

Abstract Laminated composites are being used in many engineering applications since they provide significant weight reduction, better fatigue and corrosion resistance. In this study, design optimization of a hybrid composite laminate subjected to eccentric loading was carried out using multi-objective genetic algorithm (MOGA). The ply material (carbon fiber or E glass) and fiber orientations ($-90 \leq \theta \leq 90$) were considered as design variables. The objective function was to minimize cost and weight with the maximization of the stiffness. The design constraints were the maximum Tsai-Wu failure index, first mode natural frequency. The numerical analyses were carried out by using ANSYS software package. Genetic aggregation model was used to generate the response surfaces which were used to obtain the optimum design variables. The optimum lay-up sequence and ply materials were determined for weight saving and cost reduction of hybrid composite plates. It was shown that the hybridization of carbon fiber and E glass fiber provided the optimal designs offers lower cost and higher mechanical performance. MOGA method was very effective to optimize the structural performance of the hybrid composite plates under eccentric loading.

1. Introduction

Fiber reinforced laminated composites have been used in many engineering applications due to their unique advantages such as higher specific strength/stiffness ratio, better corrosion and fatigue resistance compared to their metal counterparts. However, the reliable and economical design of these materials is much more complicated than the other traditional engineering materials since they are generally not isotropic and have many design variables that directly affects the overall structural performance [1,2].

Recently, optimization has become a vital step in the design phase of laminated composites. The structural performance of composite laminates can be optimized by tailoring fiber angle, ply thickness, number and material (hybridization) to achieve the desired requirements for different loading conditions. Therefore, many studies have been devoted to the optimum design of laminated composites. In most of these studies, fiber orientation angles and the thickness of layer were considered as design variables. Different objective functions were optimized by considering different optimization methodologies such as genetic algorithm (GA), gradient based optimization (GBM), Particle Swarm optimization (PSO). Most of the GA optimization studies in the literature focused on the optimization of the critical buckling load [3–5], maximum fundamental frequency [6–8], weight reduction [9,10], load capacity

E-mail address: bertan.beylergil@alanya.edu.tr

Peer review under responsibility of Faculty of Engineering, Alexandria University.

https://doi.org/10.1016/j.aej.2020.09.015
1110-0168

[11,12] and deformation [13–15] of composite laminates. A comprehensive review on the optimization of composite structures (beams, plates or shells) was published by Nikbakt et al. [16]. Megahed et al. [17] studied on the weight and cost optimization of hybrid natural laminated composite beams using PSO algorithm. As design variables, fiber type, fiber volume fractions, thickness, and fiber orientation angles of different layers were selected. Different boundary conditions were considered. They showed that the hybrid usage of carbon fiber and flax fiber provided the optimal designs with lightweight, low cost and higher fundamental frequencies. An et al. [18] studied on the optimal design of hybrid composite laminates made of high-stiffness skin and low-stiffness core layers. The objective was to maximize the fundamental frequency and to minimize cost by searching the optimal stacking sequences for both skin and core layers using GA. They obtained the optimal stacking sequences for hybrid composite plates made of graphite/epoxy-glass/epoxy laminated plates considering the different aspect ratios. Deveci and Artem [19] applied a fatigue life prediction model called Failure Tensor Polynomial in Fatigue (FTPF) to optimize the stacking sequence of laminated composites for improved fatigue life under various in-plane cyclic loadings. They used a hybrid algorithm (combination of genetic algorithm and generalized pattern search algorithm) to obtain the optimum discrete fiber angles which provides the highest fatigue life. Rocha et al. [20] proposed a hybrid shared/distributed memory parallel genetic algorithm formulation to deal with the optimization of laminated composite structures. The algorithm was used together with a shallow shell finite element to determine the optimal solutions for a simply supported plate and a curved panel having a circular hole. To the best of the author knowledge, a few studies in the literature focused on the application of genetic algorithms (GAs) together with finite element analysis (FEA) for the design optimization of hybrid composite laminates up to now. Further research is needed in order to provide better understanding of the finite element modeling and design optimization procedure of these hybrid composite laminates using the GAs.

In this study, a design optimization procedure based on GAs combined with the finite element method was introduced and applied to the robust design of composite hybrid laminates. Design optimization of a hybrid composite plate subjected to combined bending and torsion was carried out using multi-objective genetic algorithm (MOGA). The ply material and lay-up orientations considered as design variables. The objective function is to minimize the cost and weight of the hybrid composite with the maximization of plate stiffness. The maximum Tsai-Wu failure index, total deformation and first mode natural frequency were considered as the design constraints. The numerical analyses were carried out by using ANSYS Workbench with ANSYS Composite PrepPost (ACP) module. The numerical results were first validated against theoretical, experimental and numerical studies in the literature then the FE model was extended to the present study.

2. Theoretical

The fundamental equation, or load-deformation relation, of laminate analysis (Classical laminated plate theory, CLPT) was given in Eq. (1) as follows [21]:

$$\begin{Bmatrix} N \\ M \end{Bmatrix} = \begin{bmatrix} A & B \\ B & D \end{bmatrix} \begin{Bmatrix} \varepsilon^0 \\ \kappa \end{Bmatrix} \tag{1}$$

where $\{N\}$, $\{M\}$, $\{\varepsilon^{\circ}\}$ and $\{\kappa\}$ are the vectors of resultants forces, moments, the deformations in the midplane and the effects of curvature; respectively. [A], [D] and [B] are the extensional stiffness, bending stiffness and the coupling stiffness matrices; respectively. The coupling matrix [B], a coupling between extension and bending of the laminate, is zero for symmetrical laminates. The calculation of these matrices was given in the following equations [21]:

$$A_{ij} = \sum_{k=1}^{n} \left[\bar{Q}\right]_k (h_k - h_{k-1}) \tag{2}$$

$$B_{ij} = \frac{1}{2} \sum_{k=1}^{n} \left[\bar{Q}\right]_k (h_k^2 - h_{k-1}^2) \tag{3}$$

$$D_{ij} = \sum_{k=1}^{n} \left[\bar{Q}\right]_k (h_k^3 - h_{k-1}^3) \tag{4}$$

$$h_k = \sum_{n=1}^{k} t_k \tag{5}$$

where n, t_k and $\bar{Q}_k$ are the total number of layers, the thickness of each layer (see Fig. 1) and the transformed reduced stiffness matrix; respectively. The transformed reduced stiffness matrix ($\bar{Q}_k$) can be computed using transformation matrix (T) as follows:

$$\bar{Q}_{ij} = T^{-1} Q_{ij} T \tag{6}$$

$$T = \begin{bmatrix} m^2 & n^2 & 2mn \\ n^2 & m^2 & -2mn \\ -mn & mn & m^2 - n^2 \end{bmatrix} \text{ and } Q_{ij} = \begin{bmatrix} Q_{11} & Q_{12} & 0 \\ Q_{12} & Q_{22} & 0 \\ 0 & 0 & Q_{66} \end{bmatrix} \tag{7}$$

In Eq. (7), $m = \cos\theta$ and $n = \sin\theta$, and θ is the angle of the fiber reinforcement. The strain along the plate thickness can be calculated by using Eq. (8) as follows [21]:

$$\begin{Bmatrix} \varepsilon_x \\ \varepsilon_y \\ \gamma_{xy} \end{Bmatrix} = \begin{Bmatrix} \varepsilon_x^0 \\ \varepsilon_y^0 \\ \gamma_{xy}^0 \end{Bmatrix} + z \begin{Bmatrix} \kappa_x \\ \kappa_y \\ \kappa_{xy} \end{Bmatrix} \tag{8}$$

The CLPT constitutive equations for symmetric laminates, without in-plane forces, can be written as follows [22]:

$$\begin{Bmatrix} M_{xx} \\ M_{yy} \\ M_{xy} \end{Bmatrix} = \begin{bmatrix} D_{11} & D_{12} & D_{16} \\ D_{12} & D_{22} & D_{26} \\ D_{16} & D_{26} & D_{66} \end{bmatrix} + \begin{Bmatrix} \frac{\partial^2 w_0}{\partial x^2} \\ \frac{\partial^2 w_0}{\partial y^2} \\ 2\frac{\partial^2 w_0}{\partial x \partial y} \end{Bmatrix} \tag{9}$$

or, in inverse form

$$\begin{Bmatrix} \frac{\partial^2 w_0}{\partial x^2} \\ \frac{\partial^2 w_0}{\partial y^2} \\ 2\frac{\partial^2 w_0}{\partial x \partial y} \end{Bmatrix} = - \begin{bmatrix} D_{11} & D_{12} & D_{16} \\ D_{12} & D_{22} & D_{26} \\ D_{16} & D_{26} & D_{66} \end{bmatrix}^{-1} \begin{Bmatrix} M_{xx} \\ M_{yy} \\ M_{xy} \end{Bmatrix} \tag{10}$$

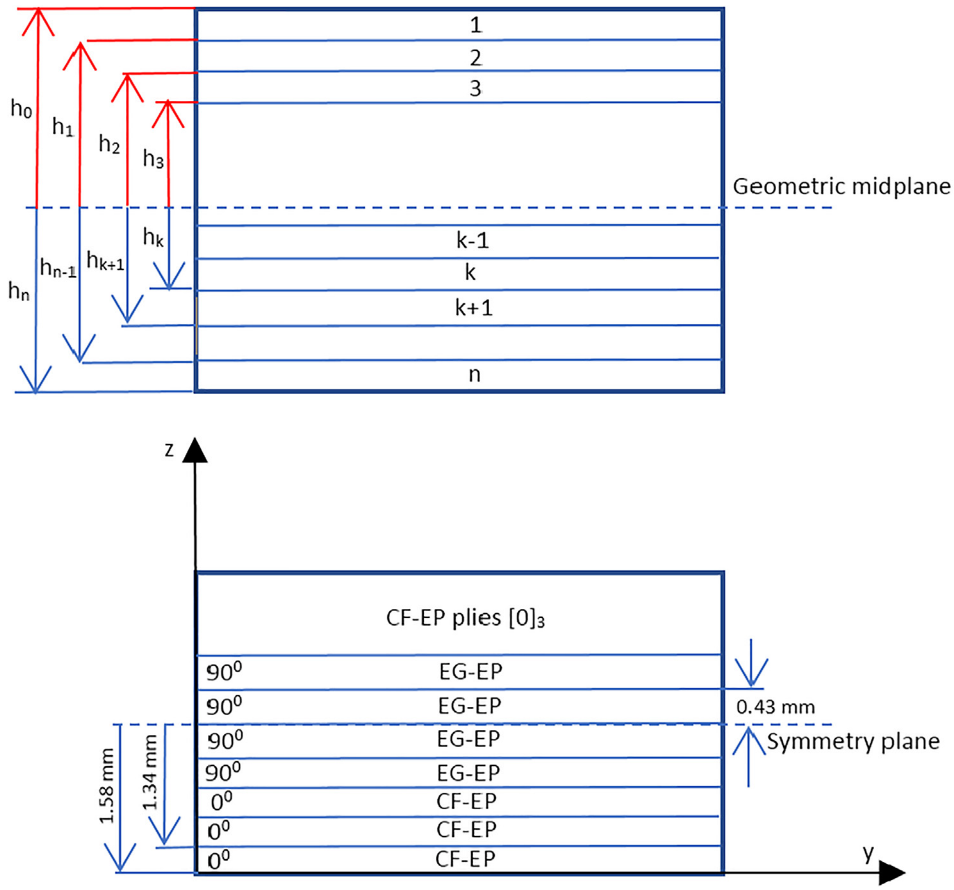

Fig. 1 Schematic illustration of the CF-EP/EG-EP hybrid composite plate.

The laminated composite plate is assumed be long enough so that the effects of the Poisson ratio and shear coupling on the deflection is negligible. In deriving the laminated beam theory, it is assumed that

$$M_{yy} = M_{xy} = 0 \tag{11}$$

Eq. (9) can be rewritten as follows;

$$\frac{\partial^2 w_0}{\partial x^2} = -D^*_{11} M_{xx} \tag{12}$$

For free vibration, the eigenvalue problem is defined in the following equation [23]:

$$\left([K] - \omega^2[M]\right)\left\{\bar{d}\right\} = 0 \tag{13}$$

where ω is the angular natural frequency in radians per second, $\{d\}$ is the mode shape, $[K]$ is the stiffness matrix and $[M]$ is the mass matrix of the system.

3. Numerical

3.1. Numerical verification

In order to validate of the numerical model, the results of present study were compared with the theoretical, experimental and numerical results obtained by other researchers. The theoretical results were obtained by using CLPT. Figueiredo [24] performed bending-torsion experiments and numerical calculations for the hybrid composite laminates composed of carbon fiber/epoxy (CF-EP) and E-glass fiber/epoxy plies (EG-EP). The authors also investigated the effects of different laminate sequences on the total deflection values of the hybrid composite laminates. Fig. 1 shows the cross-sectional view of the hybrid composite plate. The dimensions of the hybrid composite plate were 135 mm in length and 62.32 mm in width. The hybrid composite plate was composed of three CF-EP and two EG-EP symmetric plies, from the bottom to upper surface of the plate. The ply thickness of CF-EP and EG-EP were 0.24 mm and 0.43 mm; respectively. The total thickness of the hybrid composite plate was 3.16 mm. Different fiber orientations, i.e. $[0_3/90_2]_s$, $[0_2/90_2/0]_s$, $[0_4/90]_s$, $[0_2/90_3]_s$ and $[0/90/0/90_2]_s$ were considered for the verification. The mechanical properties of CF-EP and E-glass/epoxy were shown in Table 1.

Numerical analyses of the hybrid composite plate were carried out by using ANSYS Workbench with ACP module. Shell 181 (2D) and Solid 186 (3D) elements were used to create mesh structure of the hybrid composite plate. Convergence studies were carried out to determine the required element size for obtaining accurate displacement values. In total, 2108 Shell 181 elements and 29,512 Solid 186 elements were used for 2D and 3D finite element model of the hybrid composite plate; respectively. In 3D modelling, 14 elements were used through thickness direction. To simulate experimental loading scenario, two sides of the hybrid composite plate was fixed and the 50 N load (in the z direction) was applied to the plate eccentrically

Table 1 Mechanical properties of CF-EP and EG-EP composites [25].

Material	E_1 (MPa)	$E_2 = E_3$ (MPa)	$G_{12} = G_{13}$ (MPa)	G_{23} (MPa)	ν_{12} (–)	Ply thickness (mm)
CF-EP	117,840	9726	3338	2402	0.27	0.24
EG-EP	44,494	11,338	3894	2777	0.30	0.43

(4 mm away from each side). To do this, a remote point at the specific coordinates was created in ANSYS then the load was applied to the composite plate as a remote force. Fig. 2 shows the mesh structure, applied boundary/loading conditions, the fiber directions and the total deformation values obtained after static analysis. The numerical analyses were repeated for different fiber orientations; i.e. $[0_2/90_2/0]_s$, $[0_4/90]_s$, $[0_2/90_3]_s$ and $[0/90/0/90_2]_s$.

Table 2 shows the variation of the total deformation values (mm) of the hybrid composite for different laminate sequences. The number of plies at 0 and 90 degree affected the displacement values significantly. As an example, the maximum total deformation was observed in the hybrid laminates with $[0_4/90]_s$ fiber orientation (1.932 mm) whereas the minimum deformation was obtained for the $[0/90/0/90_2]_s$ hybrid laminates (0.872 mm). The loading scenario can be considered as the combination of bending and torsion. This is due the variation in the values of both *D* and *A* matrices with the fiber orientations. Table 2 also shows the comparison of the results of present study with the theoretical and published experimental and numerical results in the literature. The present predictions were very close to the published results. As stated by Figueiredo [24], a small difference was observed in the comparison of experimental and numerical results due to the manufacturing imperfections and the experimental uncertainties. The measurement of the displacement with an accuracy of 5 µm and the location of the applied load may also cause a small difference in the comparison. On the other hand, the numerical results were in good agreement with the theoretical results.

Table 3 shows the first mode natural frequency values of the hybrid composite plates. Theoretical calculations were made to determine the first-mode natural frequency value of the hybrid composite plate. As can be seen, the first-mode natural frequency values affected significantly with the variation of fiber orientations. This can be explained by the increase in D_{11} values due to different fiber orientations. It can be said that the numerical results also perfectly matched with the theoretical first-mode natural frequency analysis results. In the validation step, both 2D and 3D modelling was considered. As can be seen in Table 2 and Table 3, the predictions were very close for 2D and 3D modelling approach. Therefore, 2D modelling approach was used in the rest of this study.

3.2. Problem statement

In this study, 2D numerical analyses of a hybrid composite plate composed of CF-EP and EG-EP composite plies were

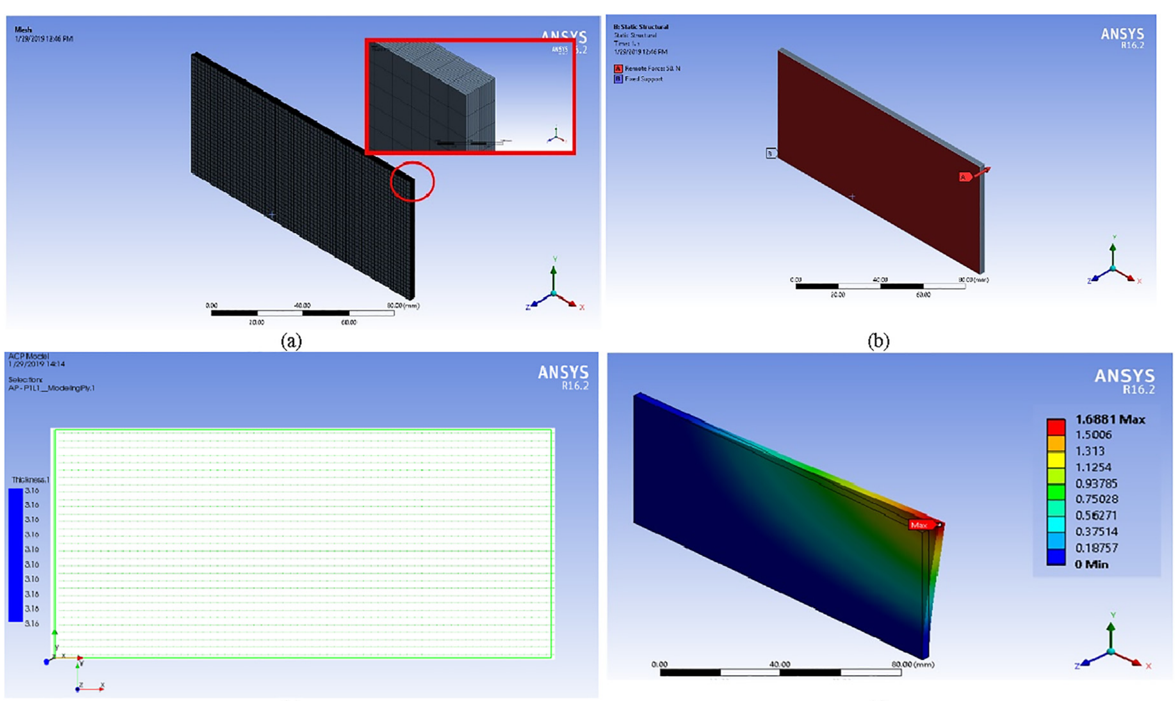

Fig. 2 (a) Mesh structure, (b) applied boundary and loading conditions, (c) fiber directions in ACP module (green arrows indicates the 0° fiber orientation, y: transverse direction) and (d) total deformation contour of the hybrid composite plate. (Laminate sequence: $[0_3/90_2]_s$). (For interpretation of the references to colour in this figure legend, the reader is referred to the web version of this article.)

Table 2 Variation of the total deformation values (mm) of the hybrid composite for different laminate sequences.

	Reference [25]		This study		
Laminate sequences[1]	Experimental	Numerical	CLPT	ANSYS (3D)	ANSYS (2D)
$[0_3/90_2]_s$	1.69	1.45	1.615	1.6881	1.6904
$[0_2/90_2/0]_s$	1.37	0.92	1.033	0.9885	0.9896
$[0_4/90]_s$	2.40	1.74	1.932	2.0678	2.0708
$[0_2/90_3]_s$	1.26	0.90	1.020	0.9718	0.9726
$[0/90/0/90_2]_s$	1.16	0.77	0.872	0.7989	0.7877

1: Hybrid configuration $[CF\text{-}EP_3/EG\text{-}EP_2]_s$.

Table 3 Variation of first mode natural frequency values (Hz) of the hybrid composite for different laminate sequence.

Laminate sequences[1]	Theoretical frequency (Hz)	ANSYS (3D)	ANSYS (2D)
$[0_3/90_2]_s$	489.78	481.03	480.61
$[0_2/90_2/0]_s$	637.94	628.07	627.64
$[0_4/90]_s$	443.39	433.99	433.58
$[0_2/90_3]_s$	642.76	633.46	633.08
$[0/90/0/90_2]_s$	712.69	702.38	702.03

1: Hybrid configuration $[CF\text{-}EP_3/EG\text{-}EP_2]_s$.

carried out using ANSYS Workbench with ACP module. The dimension of the hybrid composite plate was 120 mm in length and 60 mm in width. A force with a magnitude of 50 N was applied to the hybrid composite plate in the z-direction eccentrically. The load was applied 10 mm away from two sides of the hybrid composite. The other sides were fixed as in the case of the FE model used for the verification.

The hybrid composite plate was made of five composite plies. The thickness of each ply was assumed as 0.50 mm. Two different fiber orientations were considered; $[0/90]_s$ composed of only CF-EP plies and a hybrid configuration of $[0_{CF\text{-}EP}/90_{CF\text{-}EP}/90_{EG\text{-}EP}/0_{EG\text{-}EP}]$. The total composite thickness was 2.0 mm. The density of CF-EP and GF-EP composite were 1518 and 2000 kg/m^3; respectively. The mechanical properties of CF-EP and EG-EP composites were given in Table 4. The cost of CF-EP and EG-EP composites were assumed as 38.60 £/m^2 and 28.80 £/m^2; respectively. The weight and total cost of the composite laminates were calculated and presented in Section 6.

Fig. 3 shows the first mode natural frequency and total deformation of the hybrid composite plate with a fiber orientation of $[0_{CF\text{-}EP}/90_{CF\text{-}EP}/90_{EG\text{-}EP}/0_{EG\text{-}EP}]$. The first mode natural frequency and the total deformation of the hybrid composite plate were determined as 361.83 Hz and 5.0991 mm; respectively whereas the first mode natural frequency and the total deformation of the CF-EP composite plate with a fiber orientation of $[0/90]_s$ were determined as 440.34 Hz and 4.0996 mm; respectively.

4. Tsai-Wu failure criterion

In this study, the Tsai-Wu failure criterion was used to determine the first ply-failure in the hybrid composite laminate. The Tsai-Wu failure criterion is one of the most widely used failure criteria developed for anisotropic materials such as unidirectional composites. It has been employed to many composite engineering structures by researchers and designers over the past decades. It has also been successfully incorporated into commercial finite element software packages, such as Abaqus and ANSYS. The Tsai-Wu failure index (FI) of each composite ply can be calculated by using Eq. (14) [25]. It is assumed that the material safe if FI ≤ 1 while the first-ply failure occurs when FI$\geqslant 1$.

$$FI = F_1\sigma_1 + F_2\sigma_2 + F_3\sigma_3 + F_{11}\sigma_1^2 + F_{22}\sigma_2^2 + F_{33}\sigma_3^2 + F_{44}\sigma_4^2 + F_{55}\sigma_5^2 + F_{66}\sigma_6^2 + 2F_{12}\sigma_1\sigma_2 + 22F_{13}\sigma_1\sigma_3 + 2F_{23}\sigma_2\sigma_3 \quad (14)$$

where

$$\begin{aligned} F_1 &= \tfrac{1}{X_t} + \tfrac{1}{X_c}; F_2 = \tfrac{1}{Y_t} + \tfrac{1}{Y_c};\\ F_3 &= \tfrac{1}{Z_t} + \tfrac{1}{Z_c}; F_{11} = -\tfrac{1}{X_tX_c};\\ F_{22} &= -\tfrac{1}{Y_tY_c}; F_{33} = -\tfrac{1}{Z_tZ_c};\\ F_{44} &= \tfrac{1}{S_{23}^2}; F_{55} = \tfrac{1}{S_{13}^2};\\ F_{66} &= \tfrac{1}{S_{12}^2}; F_{12} = -\tfrac{\sqrt{F_{11}F_{22}}}{2};\\ F_{23} &= -\tfrac{\sqrt{F_{22}F_{33}}}{2}; F_{13} = -\tfrac{\sqrt{F_{11}F_{33}}}{2} \end{aligned} \quad (15)$$

In Eq. (15), X, Y and Z are the material strengths in the x, y and z directions; respectively. t and c correspond to tensile and compressive, respectively. S is the shear strength of the composite lamina. The tensile, compression and shear strength values for CF-EP and EG-EP composites were given in Table 5. Negative values indicate the compressive strength of the composites [25].

Table 4 Mechanical properties of CF-EP and EG-EP composites [27].

Material	E_1 (MPa)	$E_2 = E_3$ (MPa)	$G_{12} = G_{13}$ (MPa)	G_{23} (MPa)	ν_{12} (–)
CF-EP	123,340	7780	5000	3080	0.27
EG-EP	45,000	10,000	5000	3846.2	0.30

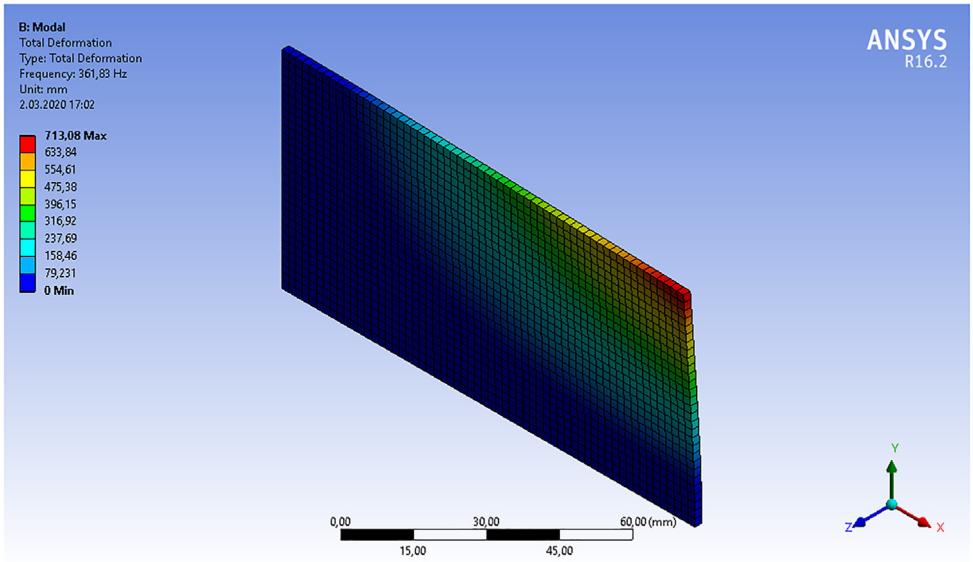

(a)

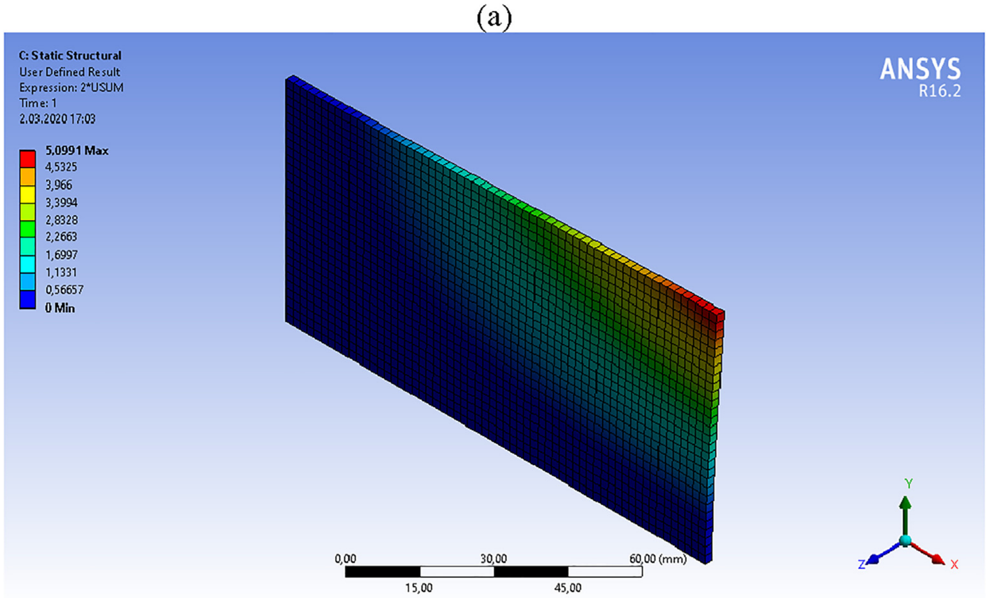

(b)

Fig. 3 (a) The first mode natural frequency and (b) total deformation values of the hybrid composite plate $[0_{CF\text{-}EP}/90_{CF\text{-}EP}/90_{EG\text{-}EP}/0_{EG\text{-}EP}]$.

Fig. 4 shows the FI contour plot for the first and the fourth plies of the hybrid composite plate. The minimum and maximum Tsai-Wu failure index were determined as 0.31317 and 0.92329; respectively. It can be said that the first ply failure will occur in the 4th ply very close to the fixed edge of the composite plates. In the case of CF-EP composites with a fiber orientation of $[0/90]_s$, the minimum and maximum Tsai-Wu failure index were determined as 0.27507 and 0.5497; respectively. The numerical results indicated the strong dependence of the natural frequency, Tsai-Wu failure index and total deformation values on the ply material and the selected fiber orientation. It is necessary to optimize these parameters in order to obtain minimum weight/cost and acceptable stiffness.

5. Multi-objective genetic algorithm

5.1. Genetic algorithm

Generally, engineering design problems require a simultaneous optimization of conflicting objectives and an associated number of constraints. Unlike single objective optimization problems, the solution is a set of points known as Pareto optimal set. Solutions are compared to other solutions using the concept of Pareto dominance. A multi-criteria optimization problem can be written as [26]:

Maximize/minimize

$$f_i(x)_i \; i = 1, ..., N \tag{16}$$

Table 5 Strength values of CF-EP and EG-EP composites [27].

Mater.	X_t (MPa)	X_c (MPa)	$Y_t = Z_t$ (MPa)	$Y_c = Z_c$ (MPa)	$S_{12} = S_{13}$ (MPa)	S_{23} (MPa)
CF-EP	1632	−704	34	−68	80	22
EG-EP	1100	−675	35	−120	80	46.15

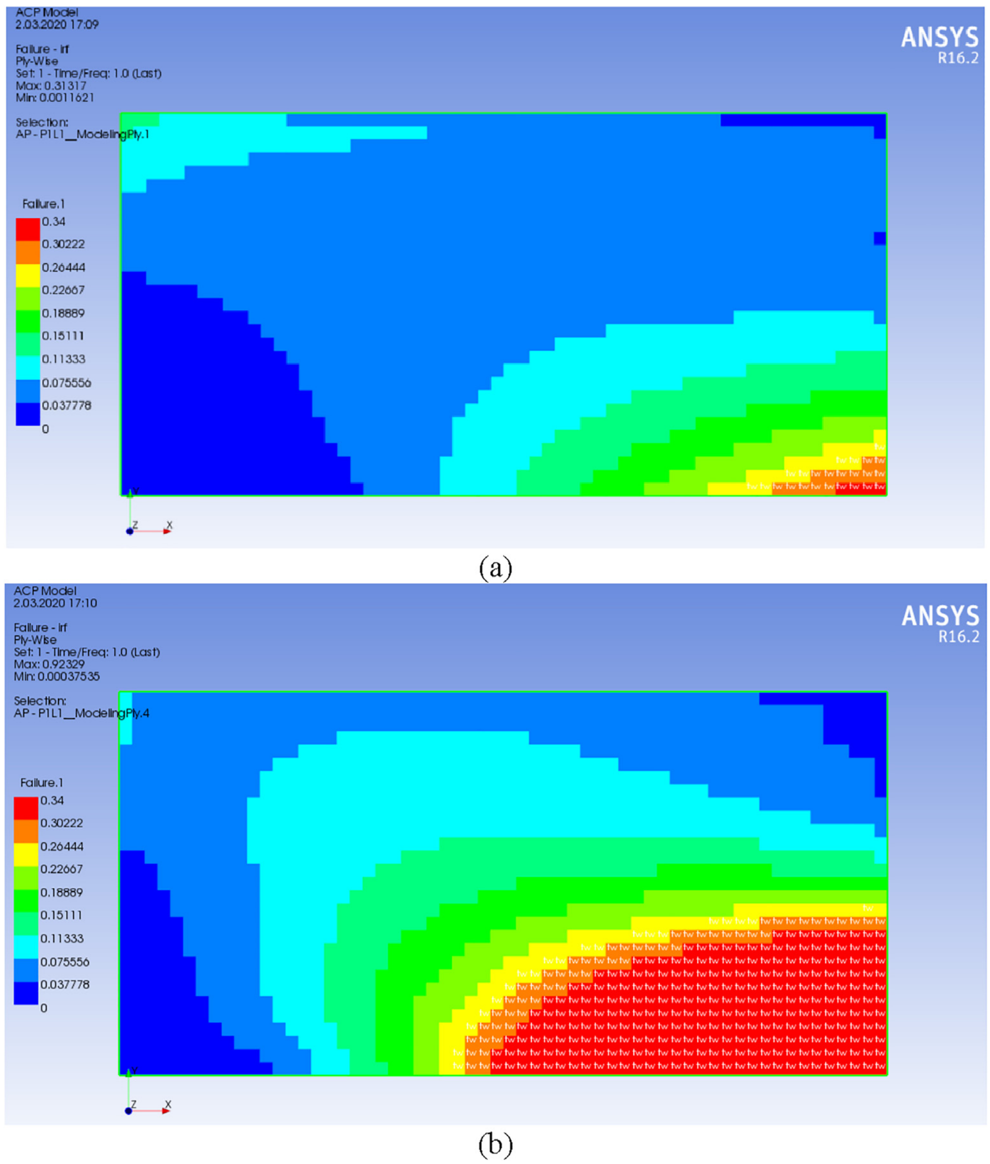

Fig. 4 Tsai-Wu failure index contour for (a) the first and (b) the fourth ply ($[0_{CF\text{-}EP}/90_{CF\text{-}EP}/90_{EG\text{-}EP}/0_{EG\text{-}EP}]$).

Subject to constraints

$$g_j(x) = 0 \; j = 1, ..., M \tag{17}$$

$$h_k(x) \leqslant 0 \; k = 1, ..., M \tag{18}$$

where f_i, g_j and h_k are the objective functions, the equality and the inequality constraints; respectively. N is the number of objective functions and x is an $n-$dimensional vector.

Genetic Algorithm (GA), a category of stochastic search methods, can be defined as search algorithms, based on the mechanics of natural selection and genetics. Genes and chromosomes are the paramount elements in GAs. A chromosome is a strand of genes. In a real-case problem, genes are the variables that should be optimized, and a chromosome is a solution to the problem. Genetic algorithms search for the optimal solution from populations of chromosomes. They have several advantages over other optimization techniques

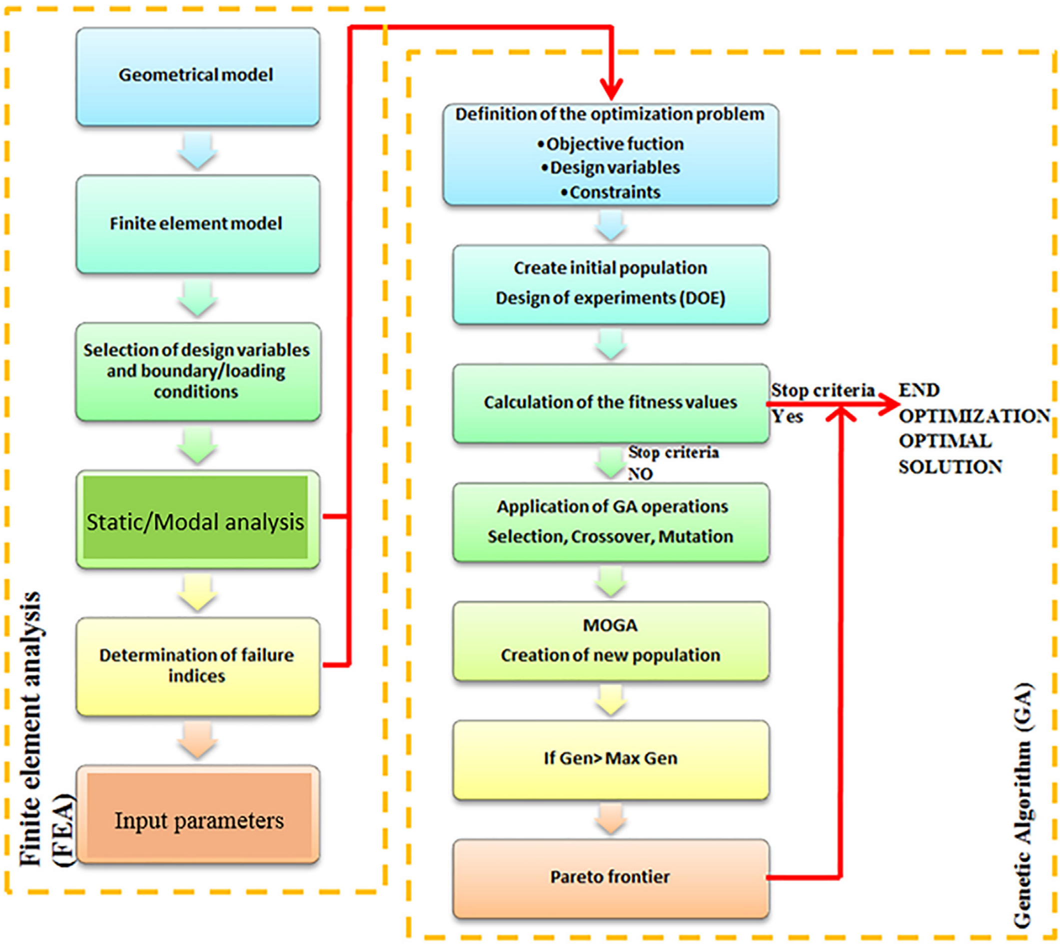

Fig. 5 Processing steps of MOGA.

as follows: They can simultaneously handle several designs and can temporarily accept worse solutions since they use probabilistic selection. Therefore, it is possible to escape from the trap of a local minima design area.

Genetic algorithms are useful tools for solving discrete problems due to easy space mapping of the design variables into genetic strings to form chromosomes. They perform a multiple directional search by maintaining a population of potential solutions. Therefore, they provide alternative solutions by performing crossover and mutation even if the best solution is not acceptable based on the considerations that have been omitted from the optimization formulation. Therefore, it is obvious that GAs is well suited for the design and optimization of laminated composite structures which possess non-linear functions of the number of plies, ply thicknesses, and orientation angles.

A Genetic Algorithm that has capabilities for multi-objective optimization is termed as Multi-Objective Genetic Algorithms (MOGAs). MOGA is a variant of the popular Nondominated Sorted Genetic Algorithm-II (NSGA-II) based on controlled elitism concepts. The processing steps of multi-objective genetic algorithm (MOGA) are shown in Fig. 5. The initial population is randomly created, and then fitness function evaluation, selection, crossover and mutation are performed. The elitism concept is introduced in order to obtain the best parents for children reproduction. When the criteria are not satisfied, the algorithm returns to initial population. And finally, the Pareto solutions are obtained.

5.2. Mathematical formulation of the optimization problem

The mathematical formulation of the optimization problem, two input-five-output problem, may be described as it follows;

Objective function
Minimize (cost, weight)
Maximize (stiffness)

Design variables
Ply angles: $-90 \leq \theta_n \leq 90$; n = 1, 2,. . ..,4
Ply material: CF-EP or EG-EP

Constraints
Tsai-Wu failure index FI $\leq$ 0.34
First mode natural frequency $\geq$ 500 Hz

The MOGA method (Multi-Objective Genetic Algorithm) was utilized to minimize cost and weight and the total deformation value of the hybrid composite laminate. The minimum factor of safety was considered as 3.0. In other words, the maximum Tsai-Wu failure index calculated for each ply should be lower than 0.333 (or equal). Two design variables were considered; ply angle and ply material. Once the static structural analysis was done, the parameters were defined using ACP module. Then, Response Surface Optimization was initiated.

Table 6 MOGA parameters used in this study.

Crossover rate	Mutation rate	Pareto percentage (%)	Number of iterations	Stability percentage
0.98	0.01	55	10	1.5195

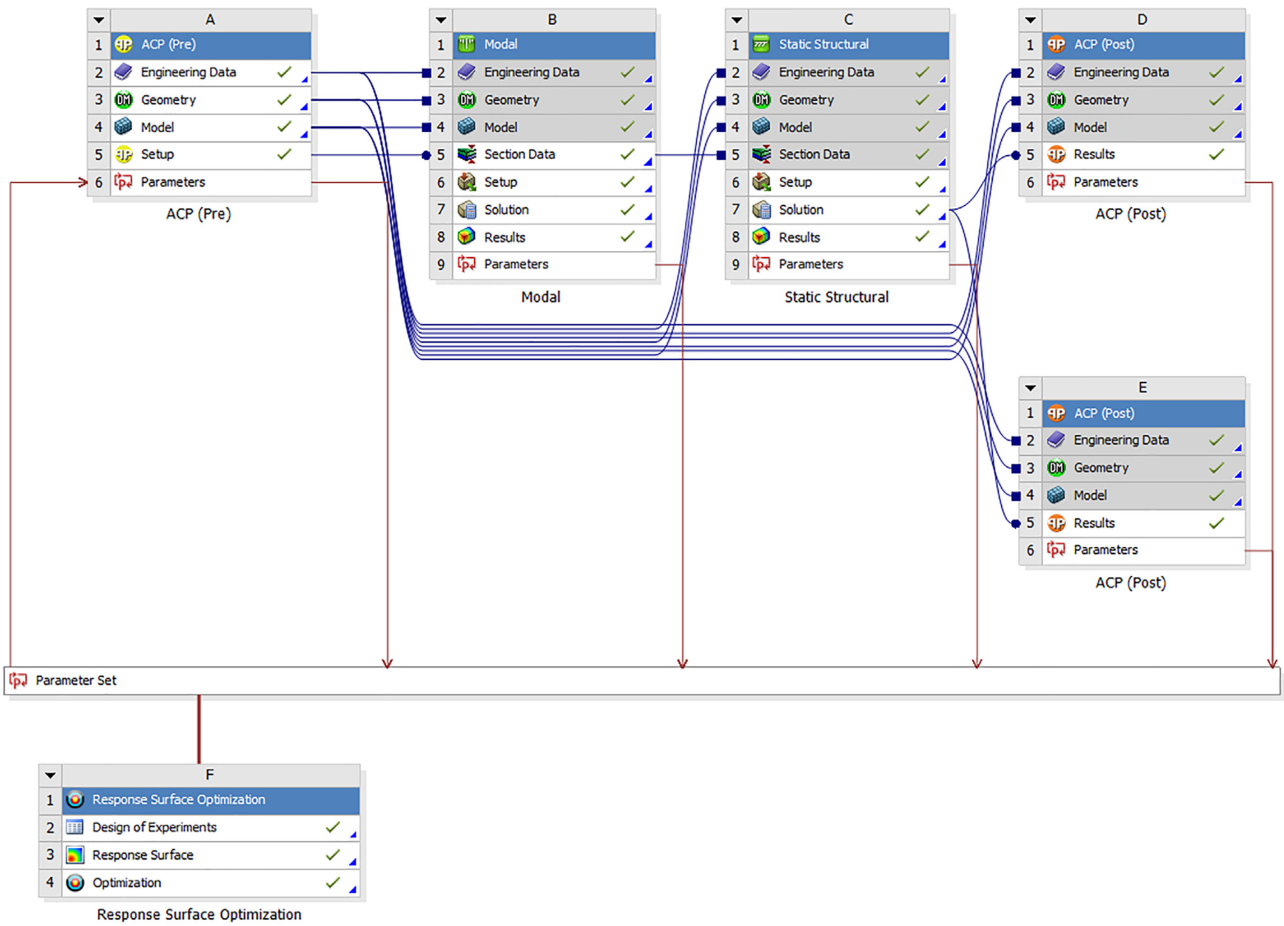

Fig. 6 Optimization flow-chart in ANSYS.

The first step was to create a design of experiments (DOE). A Central Composite Design (CCD) based DOE was setup, which created 400 Design Points for the eight input design parameters. These 400 Design Points were then run automatically to generate output data at these points.

A Mathematical formula was fitted to the data, which is called a "response surface". The parameters with significant influence on the outputs were determined from this formula, with which new response surfaces were created. Genetic aggregation metamodel was used to generate the response surface that is the most appropriate approach for each output compared to other metamodels. Table 6 shows the MOGA parameters used in this study. The MOGA was done with an initial sampling size of 10,000 samples, and with 100 samples per iteration. The maximum allowable pareto percentage which represents the ratio of the number of desired pareto points to the number of samples per iteration was 55%. When this percentage is reached, the optimization is converged. This value is generally selected between 0.55 and 0.75 for the most optimization problems. High crossover rate of 98 percent was considered to minimize premature convergence problems and low mutation rate of 1 percent was selected to prevent genetic algorithms from falling into local maxima or minima. The optimization step was converged after 10,868 evaluations and three possible candidates matching the given objectives were found. These points were verified by DOE analysis. The optimization flow-chart is shown in Fig. 6.

6. Results and discussion

6.1. Effect of fiber orientations on the stress distribution, natural frequencies and Tsai-Wu failure index

Fig. 7(a) shows the effect of fiber orientations on the equivalent stress values of CF-EP composite laminates. The fiber orientation of each ply was changed from −90 to 90 degrees with an increment of 10 degrees. The equivalent stress was almost independent of the fiber orientation of the second and third plies. The stress level was in the range of 140–150 MPa. A small increase in the stress values for the second and third plies was observed from −90 to 0 degree and 0 to 90 degree. For the second and third plies, the effect of fiber orientations was almost negligible in terms of equivalent stress. The minimum and maximum equivalent stress values were obtained for 50 and −60 degrees, respectively. Fig. 7(b) shows the effect of fiber orientations on the natural frequency values of CF-EP composite laminates. The maximum frequency values were obtained for −90 and 90 degrees as expected. The fiber orientations of the second and third plies seemed to have no significant effect on the natural frequency values. The natural frequency values were in the range of 340–370 Hz. On the other hand, the fiber orientation alteration in the first and fourth plies significantly affected the natural frequency values. In terms of the equivalent stress and natural frequency values, the first and fourth plies seemed to be more critical than the other plies of the composite laminates. It is obvious that the fiber orientation and fiber material of the top and bottom plies would be more influential on the required mechanical performance of composite laminates.

Fig. 8 show the variation of Tsai-Wu failure index values (FI) of the CF-EP composite laminate with the fiber orientations. For the first ply of the composite laminate, the minimum Tsai-Wu failure index values were obtained for the composite laminates having 45° fiber orientation. The maximum Tsai-Wu failure index were obtained when the fibers of the first ply oriented at −30 degrees. The Tsai-Wu failure index values started to increase from −90° to −30°, then the FI values decreased after passing −30 turning points. This behavior was also observed for the second ply. However, the effect of fiber orientation of second ply on the failure index was negligible as compared to other plies. For the third and fourth plies, the Tsai-Wu failure index values showed increase from −90 to 0 degree. The maximum failure index of the third ply was obtained when the fibers oriented at −45 degree whereas the minimum value was observed ±90 degree. The Tsai-Wu failure indices of the first and the fourth plies were shown to be the most affected by the fiber orientations.

Fig. 9 shows the local sensitivities among input and output parameters. The local sensitivity chart provides significant information about the impact of each input parameter on specific outputs. The output parameters-total deformation, Tsai-Wu index and first mode natural frequency values- were influenced by fiber angles.

The natural frequency values increased with the increase of the fiber orientations. The increase in fiber angle of the composite plies, except for the second ply, causes reduction in the total deformation and Tsai-Wu failure index values. It can be also noticed that the effects of fiber angle on the Tsai-Wu failure index and total deformation values were more pronounced than the natural frequency values.

6.2. Optimization results

Fig. 10 and Fig. 11 show the predicted Tsai-Wu failure index values (P16) of the composite laminate for different fiber orientations. For the first ply of the composite laminate, the minimum Tsai-Wu failure index values were obtained for the composite laminates having ±45° fiber orientation whereas

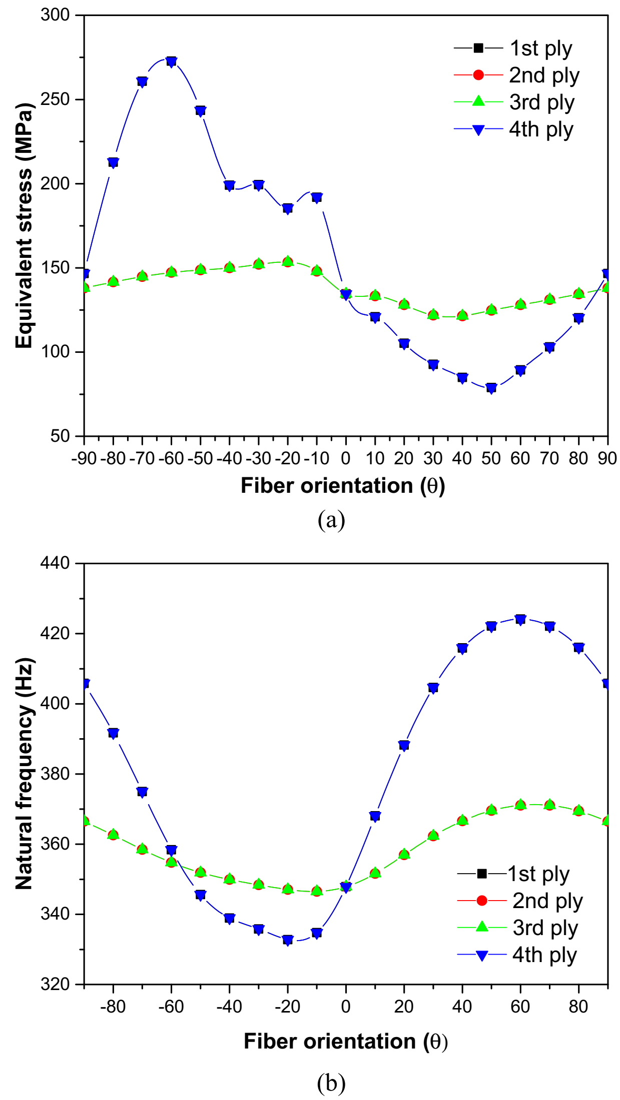

Fig. 7 The effect of fiber orientations on the (a) equivalent stress and natural frequency of CF-EP composite plates.

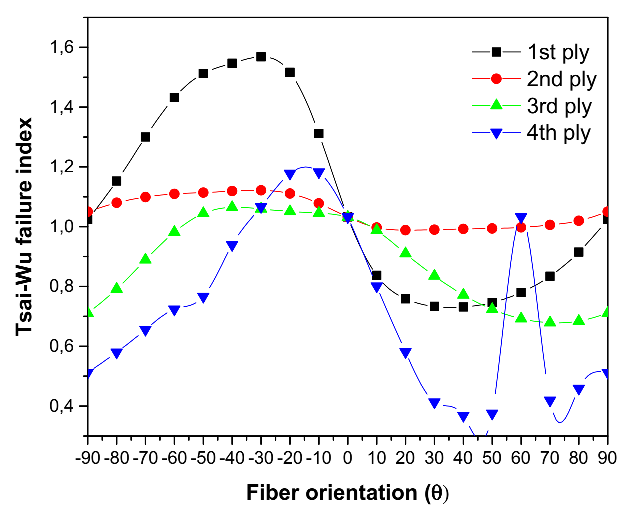

Fig. 8 The effect of fiber orientations on the Tsai-Wu failure index values of CF-EP composite plates.

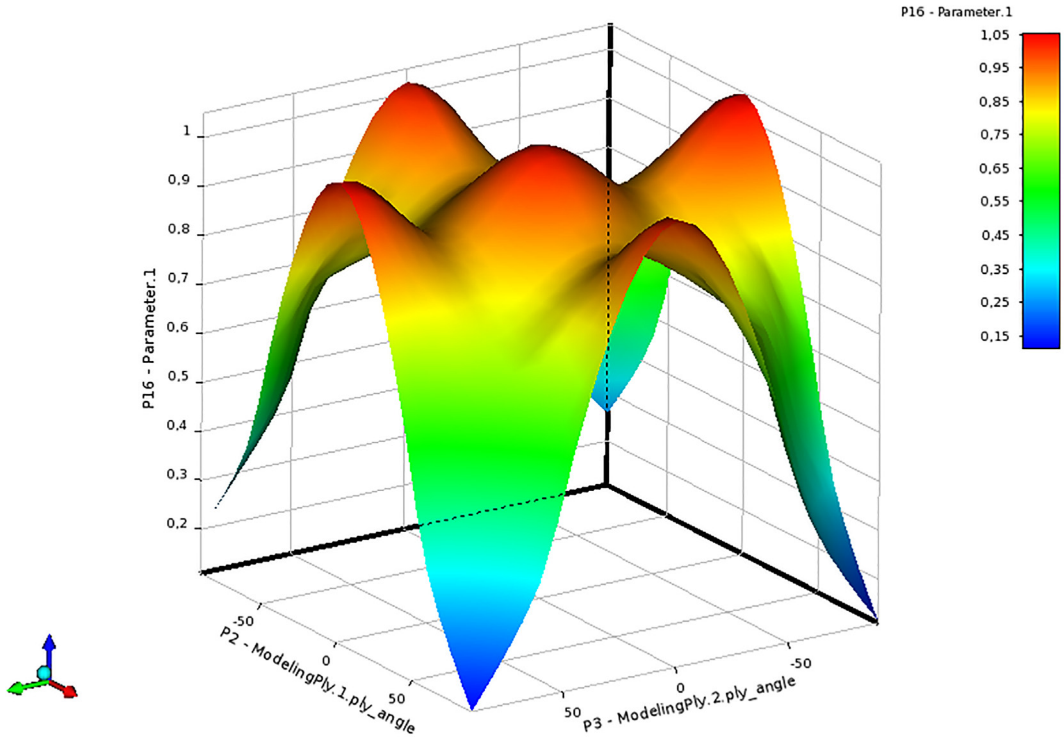

Fig. 9 The effect of fiber orientations (the first and second plies) on the Tsai-Wu failure index values.

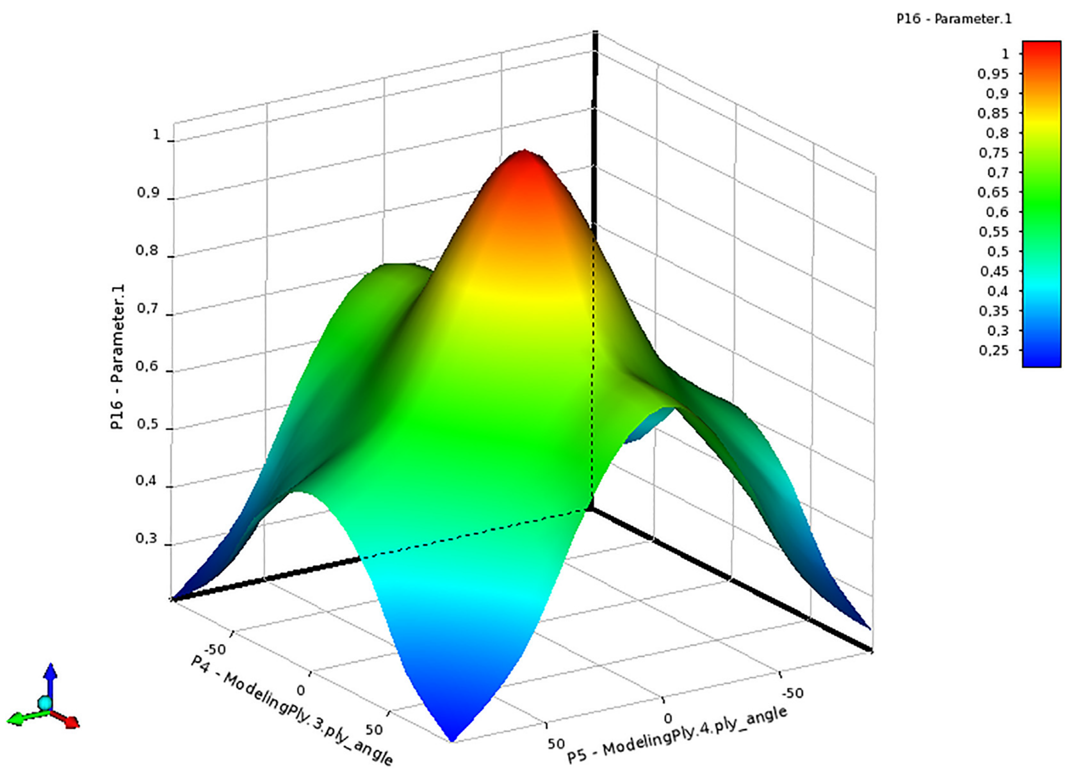

Fig. 10 The effect of fiber orientations (the third and fourth plies) on the Tsai-Wu failure index values.

the maximum Tsai-Wu failure index were obtained for 0° fiber orientation. The failure index values decrease with the increase from −90° to −45°, the FI values started to increase after passing −45/+45 turning points. This behavior was observed also for the second ply. On the other hand, in the third and fourth plies, the Tsai-Wu failure index value took its maximum value

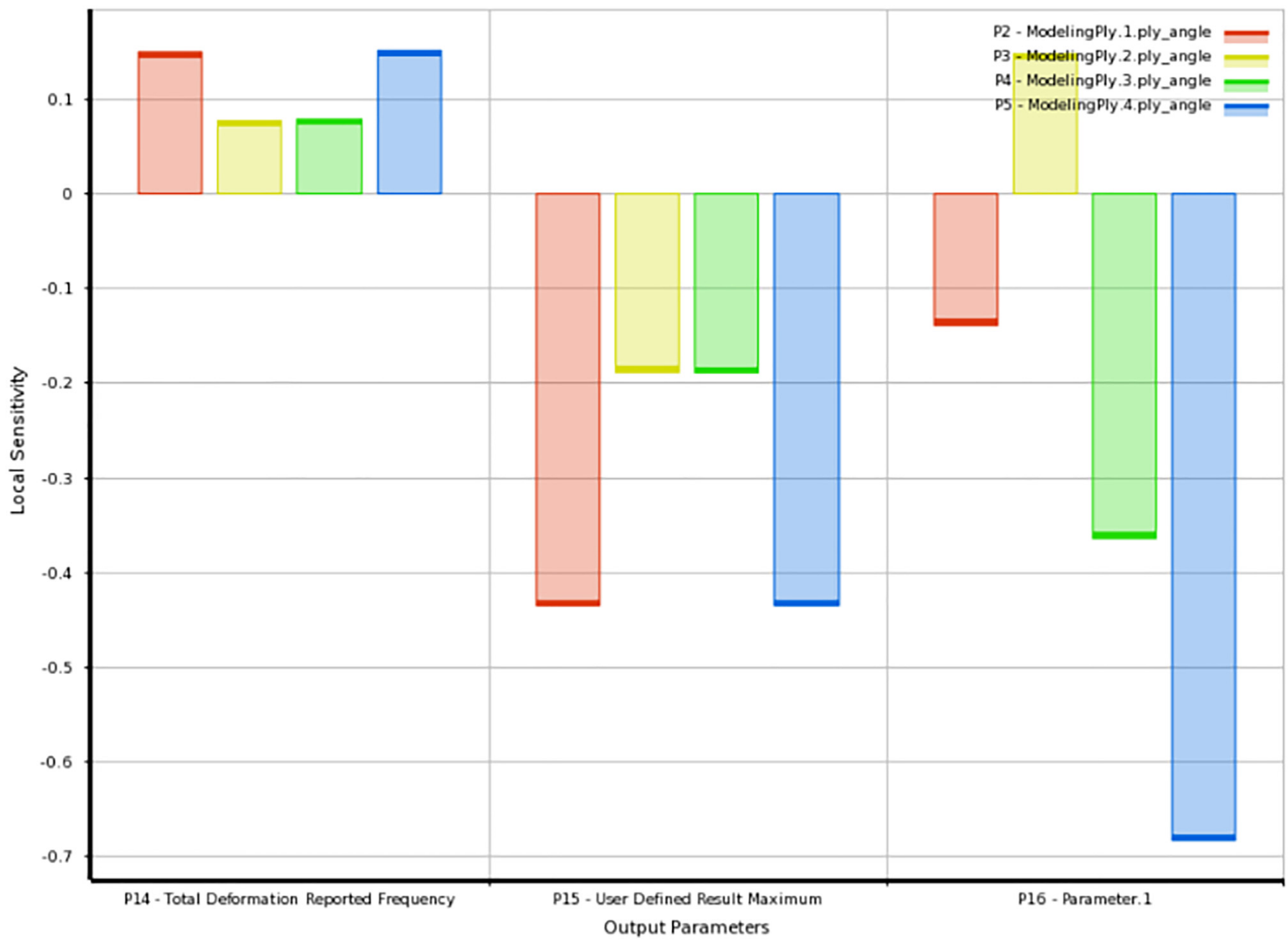

Fig. 11 Local Sensitivity of output parameters with respect to fiber orientation.

for 0° orientation whereas the minimum values were obtained for 90° orientation.

Fig. 12 shows goodness of fit for predicted vs. observed values. The quality of the approximations is directly related to the metamodel used to generate the response surface. Although some scattering was observed, the overall quality of the approximations was found to be satisfactory.

Table 7 shows the material, weight and cost values of the initial and three optimum design candidates produced by the MOGA optimization. The weight of the initial CF-EP plate and hybrid plate was determined as 21.85 and 25.33 × 10^{-6} t; respectively. The weight of the three optimum hybrid composite plates (CP-1, CP-2, CP-3) was determined as 27.06, 21.85 and 25.33 × 10^{-6} t; respectively. The cost of the three optimum hybrid composite plates (CP-1, CP-2, CP-3) was determined as 0.90, 1.11 and 0.97 £; respectively. As expected, the surface optimization predicts the variation of the weight and cost accurately. When the total number of CF-EP plies in the laminate increases, the overall weight decreases whereas the cost of the plate increases as compared to the composite laminate composed of only EG-EP plies.

The comparison of initial and optimum lamination configurations was shown in Table 8. As can be seen, the initial design configurations cannot satisfy the design constraints of the optimization problem. All configurations considered as an initial design provided lower natural frequency values than 500 Hz and higher Tsai-Wu failure index values than 0.34 except the CF-EP laminate with $[90]_4$ orientation. As expected, the highest natural frequency was obtained for the carbon fiber orientation with and orientation of $[90]_4$. The frequency values were in the range of 347–826 Hz and the stiffness of the plates with the initial design configurations was in the range of 7.7 and 46.5 N/mm. The lowest value of safety factor of the plates having initial design parameters was determined as 0.97. Table 8 shows the three optimum points obtained by MOGA. It can be noticed that all candidate points satisfied the design constraints of the optimization problem. The obtained fiber angle and material configurations provided the Tsai-Wu index lower than 0.34 and the natural frequency values higher than 500 Hz. The highest stiffness (minimum deflection) and the first mode natural frequency values for the CP-3 were obtained as 49.29 N/mm and 733.91 Hz; respectively. Among the three candidate points, the lowest Tsai-Wu failure index was determined as 0.08043. The approximate factor of safety was determined as 1/0.08043 = 12.43. Although the natural frequency value was the highest for the CF-EP laminate with $[90]_4$ orientation, the stiffness and safety factor values were less than the CP-3 laminate configuration. The stiffness and safety factor of CP-3 were higher than that of CF-EP plate with a fiber orientation of $[90]_4$ by about 7 and 12%, respectively.

Fig. 13 shows the first mode natural frequency and the Tsai-Wu failure index contour of the verified CP-3. As com-

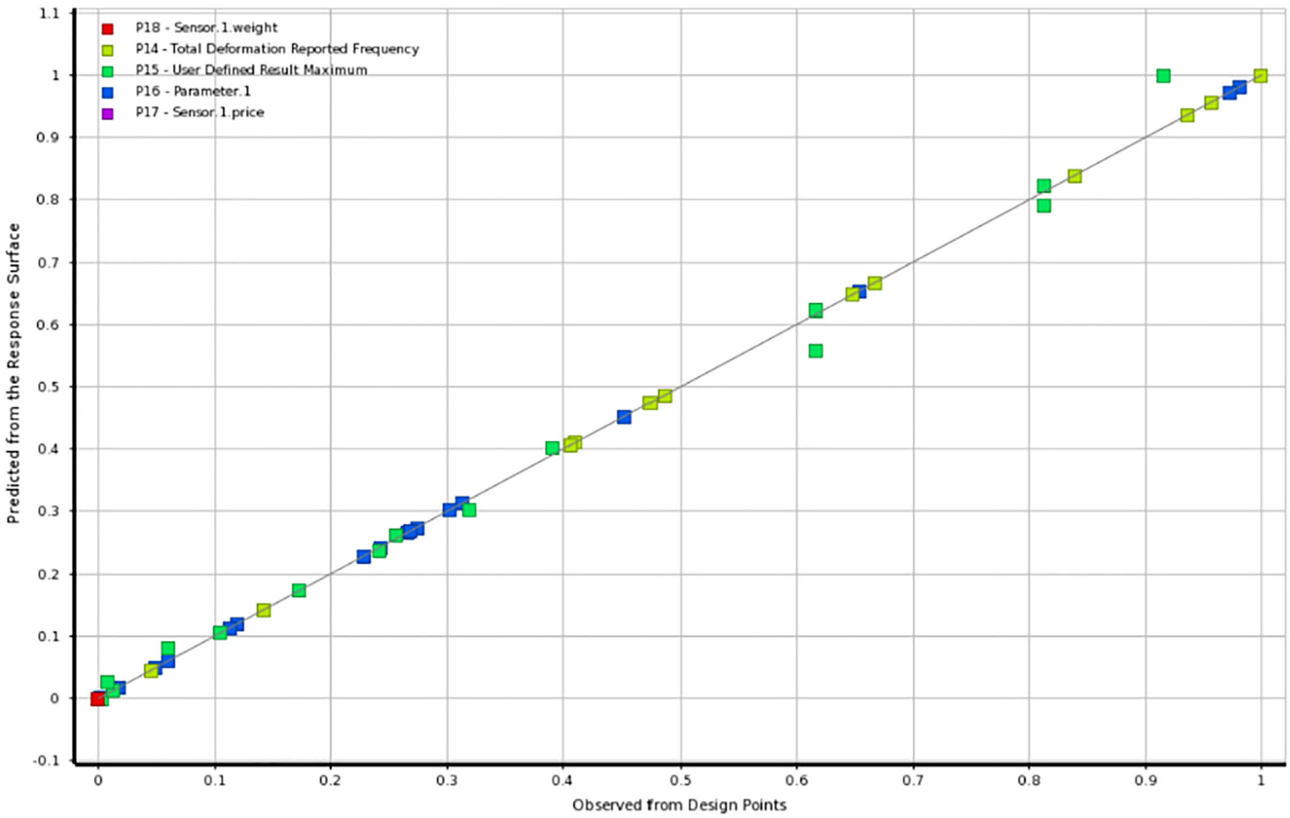

Fig. 12 Goodness of fit plot for predicted vs. FE model.

Table 7 Weight and cost values of the initial and optimum composite laminate configurations.

Laminate Configurations	Material (*)	Weight (t, 10^{-6})	Cost (£)
Initial design-CF-EP	4/4/4/4	21.85	1.11
Initial design-hybrid configuration**	4/4/5/5	25.33	0.97
Candidate Points (CP)	Material (*)	Weight (t, 10^{-6})	Cost (£)
1	5/5/5/4	27.06	0.90
2	4/4/4/4	21.85	1.11
3	4/5/5/4	25.33	0.97

*CF-EP: 4, EG-EP:5, **[$0_{CF-EP}/90_{CF-EP}/90_{EG-EP}/0_{EG-EP}$].

pared to the results for the CF-EP composite laminate with a fiber orientation of $[0/90]_s$, the first mode natural frequency was increased from 440.34 Hz to 733.91 Hz that corresponds to 66.6% increase. The stiffness of the composite plate was increased about 3 times (the total deformation decreases from 4.0996 to 1.0144) by selecting the optimum fiber angles reported in CP-3. For the optimum fiber angles, the Tsai-Wu failure index value was decreased from 0.5497 to 0.08 significantly. The factor of safety was increased from 1.82 to 12.5.

The cost of the composite plate was decreased from 1.11 £ to 0.97 £ (12.63%) with the hybridization. A small increase in the overall weight of the composite plate was observed. The weight increase due to hybridization was 16% as compared to the CF-EP composite plate with a fiber orientation of $[0/90]_{s.}$ The first mode natural frequency and the total deformation of the steel plate with a thickness of 2 mm were also

Table 8 Initial and optimum fiber orientations and the corresponding maximum Tsai-Wu failure index, the first mode natural frequency and total deflection of the composite plate.

Initial design	Ply angles	FI	Deflection (mm)	1st mode natural frequency (Hz)
CF-EP	0/0/0/0	1.0300	6.465	347.89
CF-EP	0/90/90/0	0.5497	4.096	440.34
CF-EP	90/90/90/90	0.0894	1.0732	825.51
Hybrid-case 1	$0_{CF-EP}/90_{CF-EP}/90_{EG-EP}/0_{EG-EP}$	0.9233	5.10	361.83
Hybrid-case 2	$0_{CF-EP}/90_{EG-EP}/90_{EG-EP}/0_{CF-EP}$	0.8066	5.54	350.19
Candidate Points (CP)	Ply angles	FI	Deflection (mm)	1st mode natural frequency (Hz)
1	73.29/43.56/−72.69/80.62	0.1463	1.6732	553.04
2	53.56/71.00/−19.03/−83.23	0.25713	1.8565	600.73
3	78.65/17.68/−84.27/82.96	0.08043	1.0144	733.91

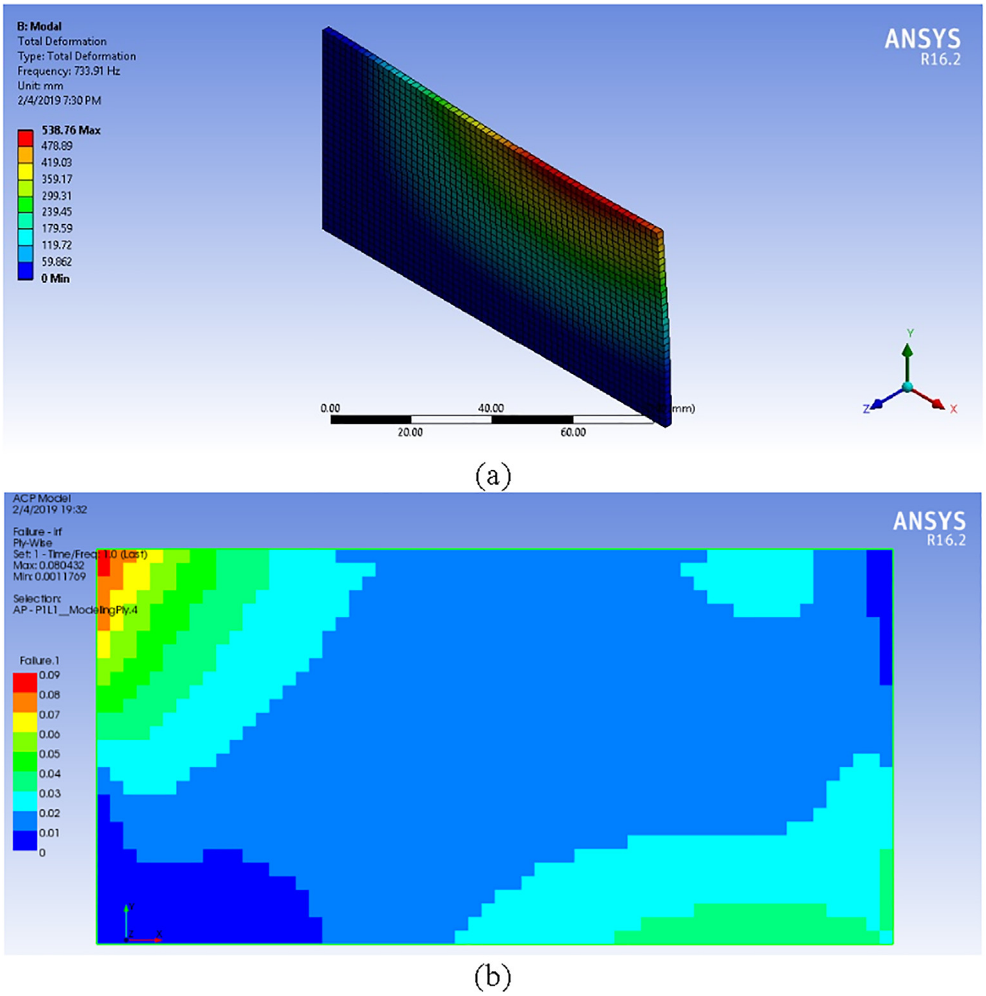

Fig. 13 (a) The first mode natural frequency and (b) Tsai-Wu failure contour of the CP-3.

determined for comparison purposes. The first mode natural frequency and the total deformation values were obtained as 576.16 Hz and 0.41225 mm; respectively. The first mode natural frequency of the CP-3 plate was 28% higher than that of steel plate. The reduction in overall weight was calculated as 78% (Weight of the steel plate: 113.04×10^{-6} t). The optimization results showed that it was possible to obtain safer composite plate with lower cost by selecting the proper fiber material and fiber orientations obtained by MOGA.

7. Concluding remarks

In this study, the design optimization of a hybrid composite laminate made of carbon and E glass fiber/epoxy plies subjected to eccentric loading was carried out by MOGA. The ply material (carbon fiber or E glass fiber) and fiber orientations ($-90 \leq \theta \leq 90$) were considered as design variables. The objective function was to minimize cost and weight with the maximization of the stiffness. The design constraints were the maximum Tsai-Wu failure index, first mode natural frequency of the composite laminate. The numerical analyses were carried out by using ANSYS Workbench with ACP module. After the verification of finite model against experimental and theoretical results available in the literature, the optimization tool in ANSYS was used to determine the optimal fiber orientations and materials. Through this optimization, the best combination of the fiber angles/materials was obtained to provide the desired structural performance for the hybrid composite plate under eccentric loading. It was shown that the hybridization of carbon fiber and E glass fiber provided the optimal designs offers lower cost and higher mechanical performance. MOGA method was shown to be effective to optimize the structural performance of the hybrid composite plates under eccentric loading.

Declaration of Competing Interest

The authors declare that they have no known competing financial interests or personal relationships that could have appeared to influence the work reported in this paper.

References

[1] H. Ghiasi, D. Pasini, L. Lessard, Optimum stacking sequence design of composite materials part I: constant stiffness design, Compos. Struct. 90 (2009) 1–11.
[2] H. Ghiasi, D. Pasini, L. Lessard, Optimum stacking sequence design of composite materials part II: variable stiffness design, Compos. Struct. 93 (1) (2010) 1–13.

[3] H.A. Deveci, L. Aydin, H. Artem, Buckling optimization of composite laminates using a hybrid algorithm under Puck failure criterion constraint, J. Reinf. Plast. Comp. 35 (16) (2016) 1233–1247.
[4] F.X. Irisarri, D.H. Bassir, N. Carrere, J.F. Maire, Multiobjective stacking sequence optimization for laminated composite structures, Compos. Sci. Technol. 69 (7) (2009) 983–990.
[5] M. Di Sciuva, M. Gherlone, D. Lomario, Multiconstrained optimization of laminated and sandwich plates using evolutionary algorithms and higher-order plate theories, Compos. Struct. 59 (1) (2003) 149–154.
[6] A.R. Vosoughi, H.D. Forkhorji, H. Roohbakhsh, Maximum fundamental frequency of thick laminated composite plates by a hybrid optimization method, Compos. Part B-Eng. 86 (2016) 254–260.
[7] Ş. Karakaya, Ö. Soykasap, Natural frequency and buckling optimization of laminated hybrid composite plates using genetic algorithm and simulated annealing, Struct. Multidiscip. O. 43 (1) (2011) 61–72.
[8] P.E. Sudhagar, A.A. Babu, V. Rajamohan, P. Jeyaraj, Structural optimization of rotating tapered laminated thick composite plates with ply drop-offs, Int. J. Mech. Mater. Des. 13 (1) (2017) 85–124.
[9] A. Gillet, P. Francescato, P. Saffre, Single-and multi-objective optimization of composite structures: the influence of design variables, J. Comp. Mater. 44 (4) (2010) 457–480.
[10] H.T. Fan, H. Wang, X.H. Chen, An optimization method for composite structures with ply-drops, Compos. Struct. 136 (2016) 650–661.
[11] G. Soremekun, Z. Gürdal, R.T. Haftka, L.T. Watson, Composite laminate design optimization by genetic algorithm with generalized elitist selection, Comput. Struct. 79 (2) (2001) 131–143.
[12] Z. Wu, P.M. Weaver, G. Raju, B.C. Kim, Buckling analysis and optimisation of variable angle tow composite plates, Thin-Walled Struct. 60 (2012) 163–172.
[13] A.A. Groenwold, R.T. Haftka, Optimization with non-homogeneous failure criteria like Tsai–Wu for composite laminates, Struct. Multidiscip. O. 32 (3) (2006) 183–190.
[14] P.E. Nicholas, K.P. Padmanaban, A.S. Sofia, Optimization of dispersed laminated composite plate for maximum safety factor using genetic algorithm and various failure criteria, Procedia Eng. 38 (2012) 1209–1217.
[15] S. Liu, Y. Hou, X. Sun, Y. Zhang, A two-step optimization scheme for maximum stiffness design of laminated plates based on lamination parameters, Compos. Struct. 94 (12) (2012) 3529–3537.
[16] S. Nikbakt, S. Kamarian, M. Shakeri, A review on optimization of composite structures Part I: Laminated composites, Compos. Struct. 195 (2018) 158–185.
[17] M. Megahed, R.M. Abo-bakr, S.A. Mohamed, Optimization of hybrid natural laminated composite beams for a minimum weight and cost design, Compos. Struct. 239 (2020) 111984.
[18] H. An, S. Chen, H. Huang, Multi-objective optimal design of hybrid composite laminates for minimum cost and maximum fundamental frequency and frequency gaps, Compos. Struct. 209 (2019) 268–276.
[19] H. Arda Deveci, H. Seçil Artem, Optimum design of fatigue-resistant composite laminates using hybrid algorithm, Compos. Struct. 168 (2017) 178–188.
[20] I.B.C.M. Rocha, E. Parente, A.M.C. Melo, A hybrid shared/distributed memory parallel genetic algorithm for optimization of laminate composites, Compos. Struct. 107 (2014) 288–297.
[21] C. Casavola, A. Cazzato, V. Moramarco, C. Pappalettere, Orthotropic mechanical properties of fused deposition modelling parts described by classical laminate theory, Mater. Des. 90 (2016) 453–458.
[22] Y. Cunedioğlu, B. Beylergil, Free vibration analysis of laminated composite beam under room and high temperatures, Struct. Eng. Mech. 51 (1) (2014) 111–130.
[23] J.S. Kumar, D. Raju, K.V.K. Reddy, Vibration analysis of composite laminated plates under higher order shear deformation theory with zig-zag function, Ind. J. Sci. Technol. 4 (8) (2011) 960–966.
[24] I.M.P. Figueiredo, Mechanical behaviour prediction and optimization of hybrid composite plates, MSc Dissertation, Technical University of Lisbon, Portugal, 2016.
[25] B. Beylergil, Y. Cunedioğlu, A. Aktaş, Experimental and numerical analysis of single lap composite joints with inter adherend fibers, Compos. Part B-Eng. 42 (7) (2011) 1885–1896.
[26] D.S. Lee, C. Morillo, G. Bugeda, S. Oller, E. Onate, Multilayered composite structure design optimisation using distributed/parallel multi-objective evolutionary algorithms, Compos. Struct. 94 (3) (2012) 1087–1096.
[27] ANSYS Inc, ANSYS User's Manual, Version 16.2, 2015.